

AD-A266 045



DOCUMENTATION PAGE

Form Approved  
OBM No. 0704-0188

2

is estimated to average 1 hour per response, including the time for reviewing instructions, searching existing data sources, gathering and  
ng the collection of information. Send comments regarding this burden or any other aspect of this collection of information, including suggestions  
Services, Directorate for Information Operations and Reports, 1215 Jefferson Davis Highway, Suite 1204, Arlington, VA 22202 4302, and to  
tuction Project (0704-0188), Washington, DC 20503.

2. Report Date.  
June 1993

3. Report Type and Dates Covered.  
Final - Journal Article

4. Title and Subtitle.

High-frequency bistatic reverberation from a smooth ocean bottom

5. Funding Numbers.

Program Element No. 0602435N/  
0601153N  
Project No. 3202/RJ035  
Task No. 030/V11  
Accession No. DN259005/  
DN294409  
Work Unit No. 5715253A3

6. Author(s).

S. Stanic, E. Kennedy, and R.I. Ray

7. Performing Organization Name(s) and Address(es).

Naval Research Laboratory  
Ocean Acoustics Branch  
Stennis Space Center, MS 39529-5004

8. Performing Organization Report Number.

JA 243:052:91

9. Sponsoring/Monitoring Agency Name(s) and Address(es).

Naval Research Laboratory  
Center for Environmental Acoustics  
Stennis Space Center, MS 39529-5004

10. Sponsoring/Monitoring Agency Report Number.

JA 243:052:91

DTIC  
ELECTE  
JUN 22 1993  
S E D

11. Supplementary Notes.

Published in The Journal of the Acoustical Society of America

12a. Distribution/Availability Statement.

Approved for public release; distribution is unlimited.

12b. Distribution Code.

13. Abstract (Maximum 200 words).

High-frequency bistatic reverberation was measured from a smooth, sandy, featureless bottom located 19 miles south of Panama City, FL. Bistatic scattering variability is presented as a function of frequency (20-180 kHz), grazing angles (9.5°-30°), and small horizontal and vertical bistatic scattering angles. Results show that bistatic variabilities tend to decrease with decreasing grazing angles and decreasing source beamwidths. Possible explanations for these decreasing variations are also presented.

93-13838



14. Subject Terms.

Sea Floor Roughness, Ocean Bottom Scattering, High-Frequency Acoustic

15. Number of Pages.

6

16. Price Code.

17. Security Classification of Report.

Unclassified

18. Security Classification of This Page.

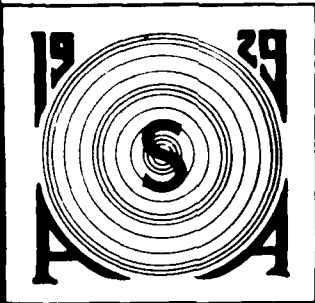
Unclassified

19. Security Classification of Abstract.

Unclassified

20. Limitation of Abstract.

SAR



Reprinted from

# THE JOURNAL

of the

# Acoustical Society of America

Vol. 93, No. 5, May 1993

## High-frequency bistatic reverberation from a smooth ocean bottom

S. Stanic, E. Kennedy, and R. I. Ray

*Naval Ocean and Atmospheric Research Laboratory, Ocean Acoustics Division, Stennis Space Center,  
Mississippi 39529-5004*

pp. 2633-2638

Accession For	
NTIS CR&I	<input checked="" type="checkbox"/>
DTIC TAB	<input type="checkbox"/>
Unannounced	<input type="checkbox"/>
Justification	
By _____	
Distribution/	
Availability Codes	
Dist	Avail and/or Special
A-1	20

# High-frequency bistatic reverberation from a smooth ocean bottom

S. Stanic, E. Kennedy, and R. I. Ray

Naval Ocean and Atmospheric Research Laboratory, Ocean Acoustics Division, Stennis Space Center,  
Mississippi 39529-5004

(Received 17 July 1992; accepted for publication 23 December 1992)

High-frequency bistatic reverberation was measured from a smooth, sandy, featureless bottom located 19 miles south of Panama City, FL. Bistatic scattering variability is presented as a function of frequency (20–180 kHz), grazing angles (9.5°–30°), and small horizontal and vertical bistatic scattering angles. Results show that bistatic variabilities tend to decrease with decreasing grazing angles and decreasing source beamwidths. Possible explanations for these decreasing variations are also presented.

PACS numbers: 43.30.Gv, 43.30.Ma, 43.30.Hw

## INTRODUCTION

Active high-frequency shallow-water sonar applications require high-resolution characterizations of ocean bottom reverberation, including estimates of both monostatic and bistatic scattering strengths. Bistatic scattering may be the dominant mechanism that degrades interelement and interbeam receiver coherence that sets limits on array processing gain.

High-frequency bottom scattering as a function of frequency, grazing angle, pulse length, and environmental conditions have been reported by numerous authors.<sup>1–6</sup> However, these authors have not reported any bistatic results. Nolle *et al.*<sup>7</sup> made a series of scattering measurements in a sand-filled tank using separate transmitting and receiving systems but reported only monostatic results. Urick<sup>8,9</sup> conducted a series of bistatic measurements in two areas off the coast of Florida. In both areas, Urick found that bistatic scattering showed little dependence on bistatic angles. A series of small angle bistatic measurements taken east of Jacksonville, FL, was reported by Stanic *et al.*<sup>10</sup> These results also showed little dependence of bistatic scattering on bistatic angles. However, variations in bistatic scattering strength decreased with decreasing grazing angles. A weak bistatic scattering frequency dependence was also reported.

Zabul *et al.*<sup>11</sup> and Martin<sup>12</sup> conducted a series of theoretical investigations into the angular and frequency spreading of an acoustic field scattered from a rough surface. Neither Zabul nor Martin compared their results to experimental data. Recently, Restrepo and McDaniel<sup>13</sup> developed two spatial covariance models and compared their out-of-plane scattering results using flat surfaces and rough surfaces with Gaussian roughness spectra. Comparison of intensity was good only if the surface was very rough, or the direction specular. The results were presented for large bistatic angles and made no data comparisons. Ellis and Crowe<sup>14</sup> calculated bistatic reverberation using a three-dimensional scattering function but made comparisons only to measured low-frequency, deep-water reverberation.

This paper presents high-frequency small angle bistatic scattering results from an experiment conducted in a flat sandy area 19 miles south of Panama City, FL. These mea-

surements were made as a function of frequency (20–180 kHz), grazing angle (9.5°–30°), and small horizontal and vertical bistatic scattering angles. Levels at each hydrophone were compared to levels at a reference hydrophone and the difference presented as horizontal and vertical scattering strength variations. Monostatic scattering strength results are given in Ref. 15. These bistatic results are compared to similar bistatic results reported by Stanic *et al.*<sup>10</sup> Possible explanations for the observed results are also presented.

## I. EXPERIMENTAL MEASUREMENTS

The experimental area was located using side scan sonar surveys and underwater television scans. Small-scale features of the experimental site were characterized using data provided by stereophotography and sediment core analysis. These techniques are outlined in Ref. 16. Bistatic scattering measurements were made using a 12 hydrophone two-dimensional spatial receiving array and a pair of nonlinear parametric sources. The orientation of the receiving array and sources were controlled by a three-axis positioning system. The positioning system was mounted on top of a 7.6-m-high undersea tower. Figure 1 shows the configuration of the transmitting and receiving arrays. The 450-kHz source transmitted difference frequencies between 180 and 90 kHz/WB (widebeam). The 250-kHz source transmitted difference frequencies between 90 kHz/NB (narrow beam) and 20 kHz. Beamwidths for both sources are given on Table I. Source levels ranged from 180 dB  $r_0^{-1}$   $\mu$ PA at 20 kHz to 214 dB  $r_0^{-1}$   $\mu$ PA at 180 kHz. The measurements were made using 5-ms-long cw pulses. The receiving hydrophones were EDO model 6660 omnidirectional units with integrated filters and preamplifiers. Data from each of the 12 hydrophones were base banded to 5 kHz and simultaneously digitized at 20 kHz. For each hydrophone channel and experimental configuration, 50 scattered signal envelopes were averaged, a mean envelope level was estimated and the standard deviation calculated.

Figure 2 is a schematic of the horizontal and vertical scattering geometry. The range along the maximum response axis (MRA) of the sources is given by  $R$ . Here,  $R_x$  and  $R_y$  are the ranges between the hydrophones and the

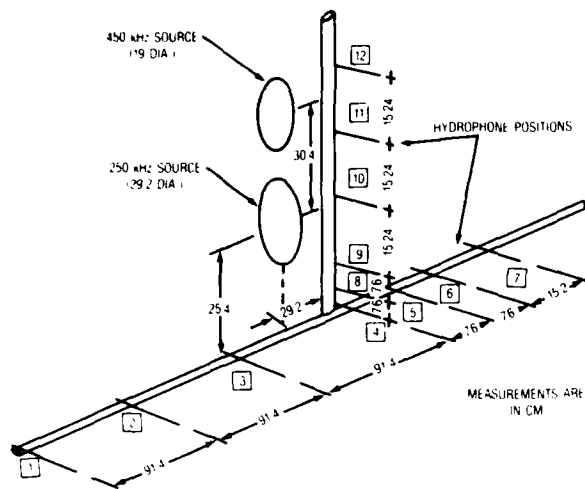


FIG. 1. Source and receiver array configurations.

estimated center of the insonified area ( $A$ ). The horizontal and vertical bistatic scattering angles are given by  $\theta_{\pm h}$  and  $\theta_{\pm v}$ . The sign designates which side of the source MRA a hydrophone is located. The grazing angle is given by  $\theta_g$ . The average bistatic scattering strength is given by

$$BS = RL - SL - TL_1 - TL_2 - 10 \log A,$$

where  $RL$  is the average received level,  $SL$  is the source level at 1 m along the MRA,  $TL_1$  is the transmission loss along  $R$ ,  $TL_2$  the transmission loss along  $R_h$  or  $R_v$ , and  $A$  is the insonified area.

For data taken in the horizontal plane, the level at hydrophone 4 was used as the reference level. This hydrophone was located closest to the vertical axis of both sources. For data taken in the vertical plane at frequencies between 180 kHz and 90 kHz/WB (450-kHz source) and at a grazing angle of  $30^\circ$ , the reference hydrophone was number 11. For all other vertical measurements, the reference hydrophone was number 10.

## II. EXPERIMENTAL RESULTS

The experimental area was a large homogeneous, featureless, hard-packed sandy bottom. Figure 3 is a photograph of the experimental area. The average sediment properties are given in Table II. Figure 4 shows two results

TABLE I. Source beamwidths as a function of frequency

	Frequency (kHz)	Beamwidth ( $-3$ dB)
250-kHz source	20	2.5
	40	2.0
	60	1.5
	90 WB	1.2
450-kHz source	90 WB	2.75
	10	2.2
	150	2.0
	180	2.0

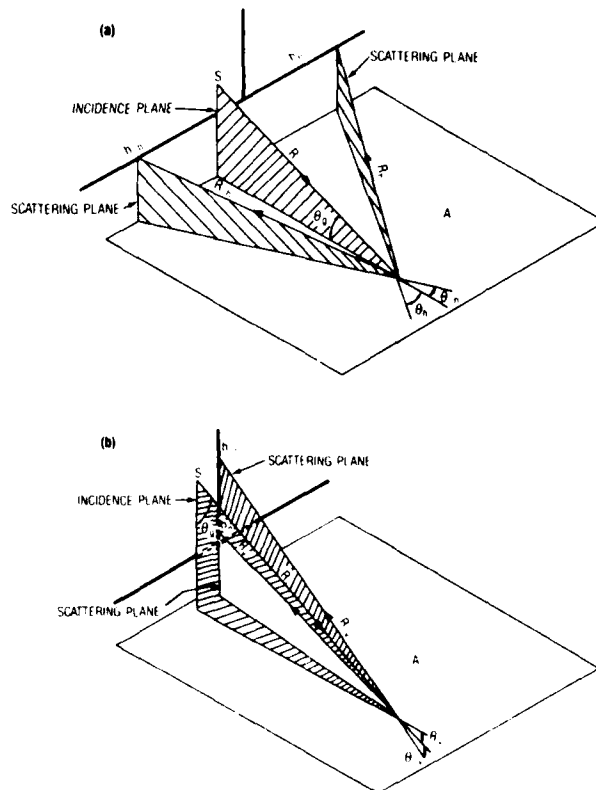


FIG. 2. Horizontal and vertical bistatic scattering geometry.

of bottom roughness spectra ( $S$ ) from the analysis of the stereophotographs. These spectra represent the extremes in bottom roughness that were present in the experiment area. These spectra have  $f^{(1.22)}$  and  $f^{(1.81)}$  frequency dependencies. This 0.42 range of dependencies is about half the range measured during the Jacksonville experiments.



FIG. 3. Typical photograph showing the smooth bottom at the experimental site ( $58 \times 27$  cm).

TABLE II. Average values of sediment parameters in the upper 20 cm.

Velocity ratio	1.133
Porosity	39.0%
Mean grain size (mm)	0.166
Compressional wave attenuation at 400 kHz	234.0 dB/m

**A. Horizontal bistatic scattering**

Figure 5 shows the measured high-frequency horizontal bistatic scattering variations as a function of frequency (180, 150, 110, and 90 kHz/WB), grazing angle (30°, 20°, and 9.5°), and small horizontal bistatic scattering angles (-10.2° to 1.14°). These measurements were made using the 450-kHz source. The data points are at the positions of the receiving hydrophones measured as a function of bistatic angles. The data at each bistatic angle are the differences between the average level at that hydrophone and the average level at the reference hydrophone located closest to the maximum response axis of the source. This reference hydrophone was labeled as 0°. For clarity, the horizontal scale for positive bistatic angles has been expanded. At a grazing angle of 30° the bistatic variations are between 8.2 and -12.5 dB. The variations are between 3.5 and -13.3 dB at a grazing angle of 20° and between 8.8 and -8.8 dB at a grazing angle of 9.5°.

Figure 6 shows the low-frequency (90 kHz/NB, 60, 40, and 20 kHz) horizontal bistatic scattering variations as a function of grazing angles (30°, 20°, and 9.5°) and bistatic

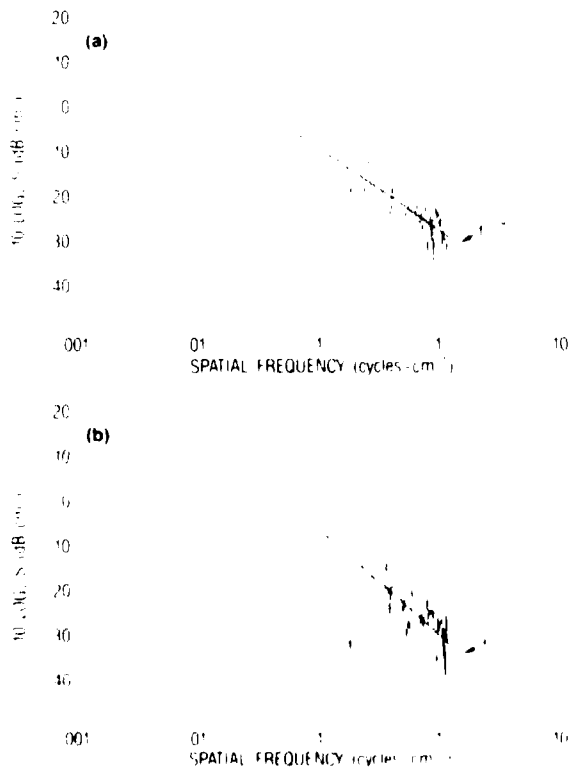


FIG. 4. Surface roughness spectra for two different areas

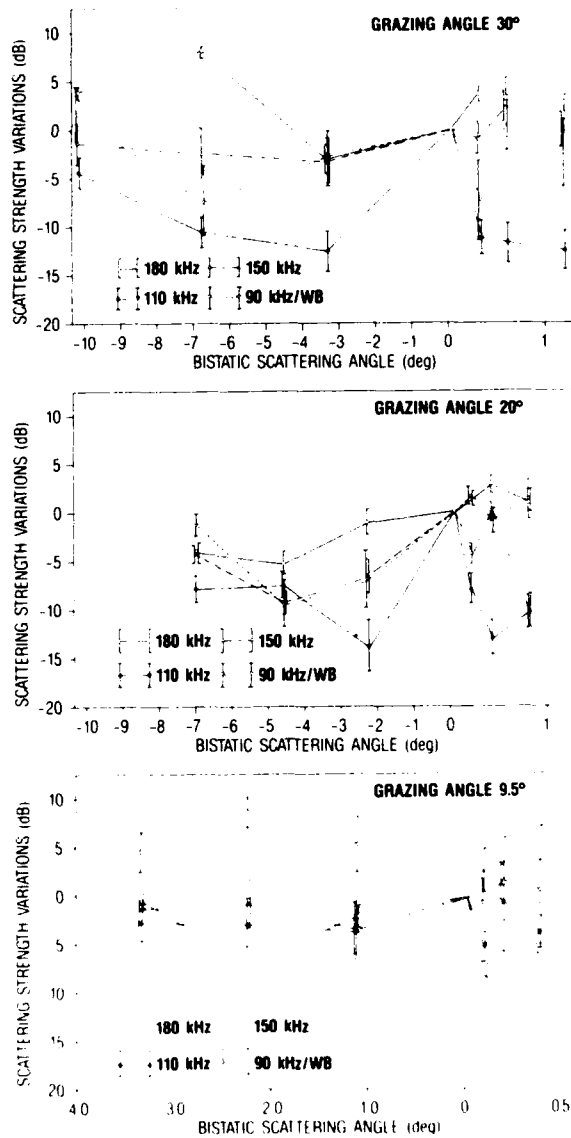


FIG. 5. High-frequency horizontal bistatic scattering variations

scattering angles (-10.2° to 1.14°). These measurements were taken using the 250-kHz source. The horizontal scale has again been expanded for positive bistatic angles. At 30°, the bistatic variations were between 8.4 and -14.0 dB. At grazing angles of 20° and 9.5° the bistatic variations were between 7.1 and -9.9 dB and between 3.6 and -6.7 dB, respectively. Low source levels at 20 kHz did not allow for consistent bistatic measurements at a grazing angle of 9.5°.

Figure 7 shows the range of horizontal bistatic scattering variations as a function of frequency and grazing angle (the 90-kHz/WB data was used). The frequency dependence of these variations is -0.03, 0.04, and 0.01 dB/kHz for grazing angles of 30°, 20°, and 9.5°, respectively.

The error bars shown in Figs. 5, 6, and all others are the standard deviations of the measured data. Since a stable platform was used, the ping-to-ping fluctuations in the

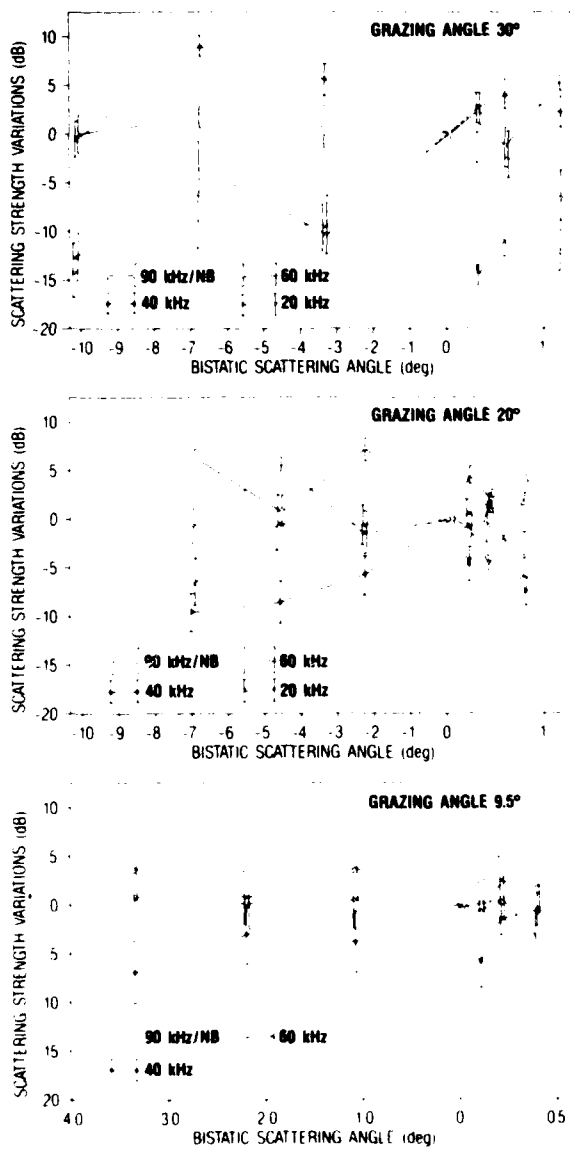


FIG. 6. Low-frequency horizontal bistatic scattering variations.

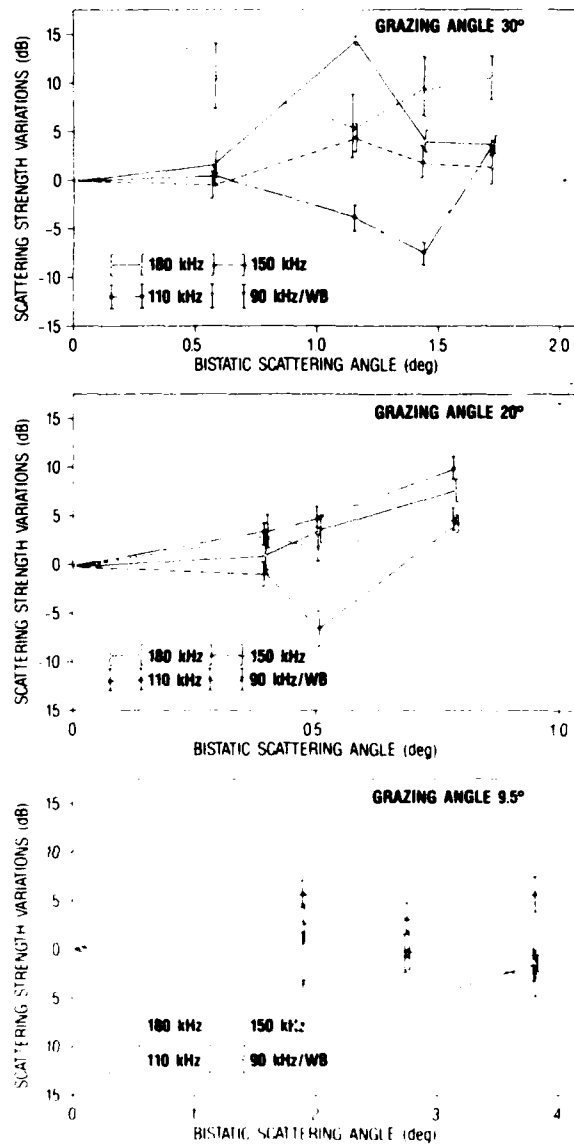


FIG. 8. High-frequency vertical bistatic scattering variations.

measured data were due to small fluctuations in the index of refraction of the water column. These fluctuations cause small displacements in the position of theinsonified areas resulting in ping-to-ping envelope level variations. No standard deviations are shown for the reference hydrophones.

### B. Vertical bistatic scattering

Figure 8 shows the high-frequency vertical bistatic scattering variations as a function of frequency (180, 150, 110, and 90 kHz/WB), grazing angles, (30°, 20°, 9.5°), and small vertical bistatic angles (0.57° to 1.71°). At a grazing angle of 30° the vertical bistatic scattering variations are between 14.5 and -7.1 dB. This range is 0.9 dB greater than the horizontal variations at 30°. At the 20° grazing angle, the vertical variations are between 10.6 and -6.3 dB. This range is 0.1 dB larger than the corresponding

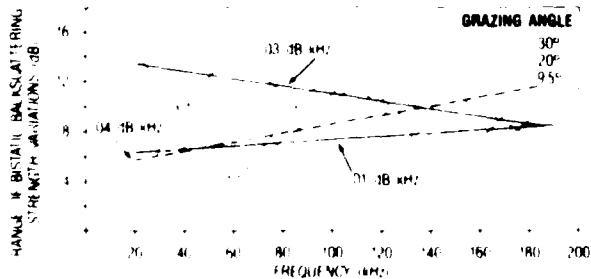


FIG. 7. Range of horizontal bistatic scattering variations.

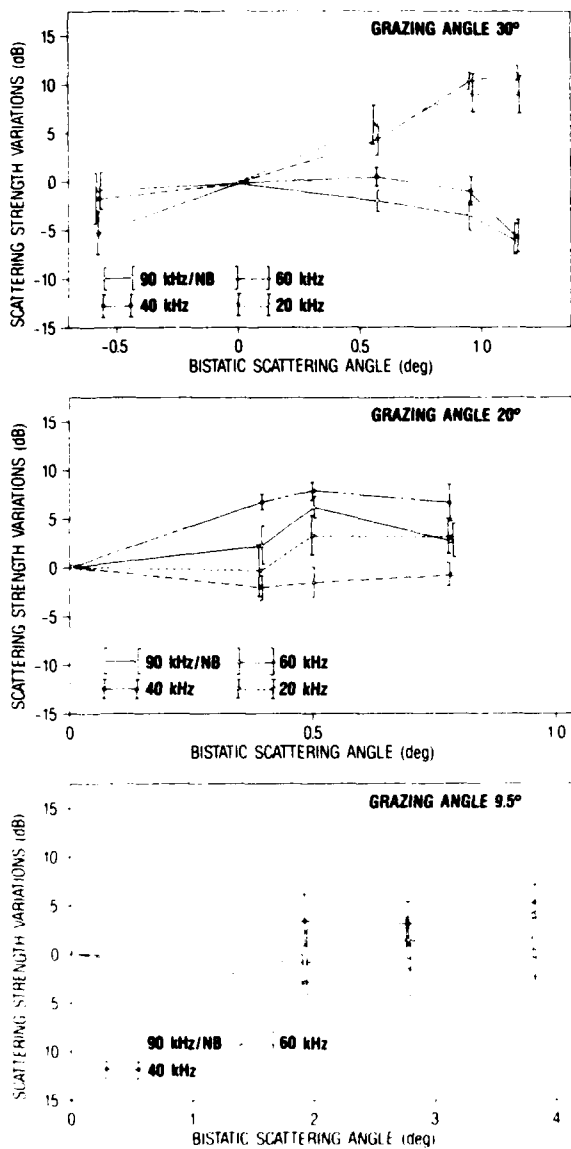


FIG. 9. Low-frequency vertical bistatic scattering variations

horizontal variations. The vertical variations at a grazing angle of  $9.5^\circ$  are between 5.9 and  $-5.2$  dB. This range is 6.5 dB smaller than the horizontal variation at  $9.5^\circ$ .

The low-frequency (90 kHz/NB, 60, 40, and 20 kHz) vertical bistatic variations as a function of grazing angles ( $30^\circ$ ,  $20^\circ$ ,  $9.5^\circ$ ), and bistatic angles are shown in Fig. 9. At a grazing angle of  $30^\circ$ , the vertical variations are between 10.6 and  $-5.7$  dB. This is 1.8 dB less than the corresponding low-frequency horizontal variations. The variations at grazing angles of  $20^\circ$  and  $9.5^\circ$  are between 7.7 and  $-2.1$  dB and 5.4 and  $-2.8$  dB, respectively. These variations are 7.2 and 2.1 dB less than the horizontal variations at  $20^\circ$  and  $9.5^\circ$ .

The range of vertical bistatic variations as a function of frequency and grazing angle is shown in Fig. 10 (the 90-kHz/WB data were used). The frequency dependence at

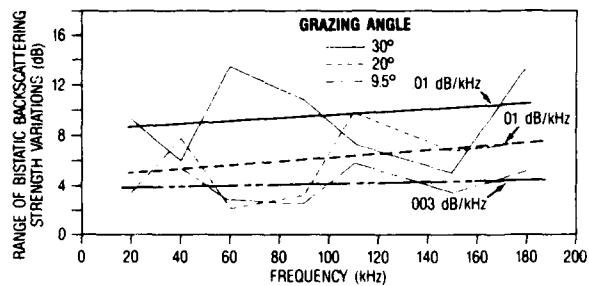


FIG. 10. Range of vertical bistatic scattering variations.

grazing angles of  $30^\circ$ ,  $20^\circ$ , and  $9.5^\circ$  are 0.01, 0.01, and 0.003 dB/kHz, respectively.

### C. Beamwidth dependence

Figure 11 shows the beamwidth dependence of the horizontal bistatic scattering variations for a source frequency of 90 kHz. At 90 kHz/NB, the 250-kHz source had a beamwidth of  $1.2^\circ$  and at 90 kHz/WB the 450-kHz source had a beamwidth of  $2.75^\circ$ . The horizontal scale was again expanded for positive bistatic angles. In general, the bistatic scattering variations measured using the narrow-beam source were less than those measured using the widebeam source.

The vertical bistatic variations at 90 kHz as a function of beamwidth and grazing angle are shown in Fig. 12. At a grazing angle of  $30^\circ$ , the variations using the narrow-beam source were significantly less than those measured using the widebeam source. At grazing angles of  $20^\circ$  and  $9.5^\circ$ , the differences were very small.

### III. DISCUSSION

In this paper, we have addressed small-angle, high-frequency, bistatic bottom scattering. Our results have shown that unlike the horizontal results measured at Jacksonville,<sup>10</sup> the range of horizontal bistatic scattering varia-

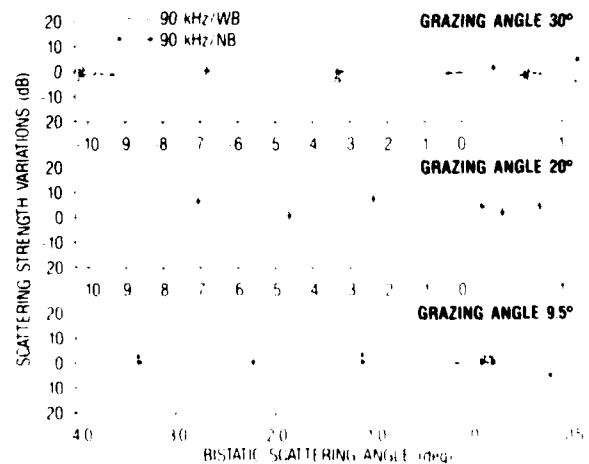


FIG. 11. Beamwidth dependence of horizontal bistatic scattering variations at 90 kHz

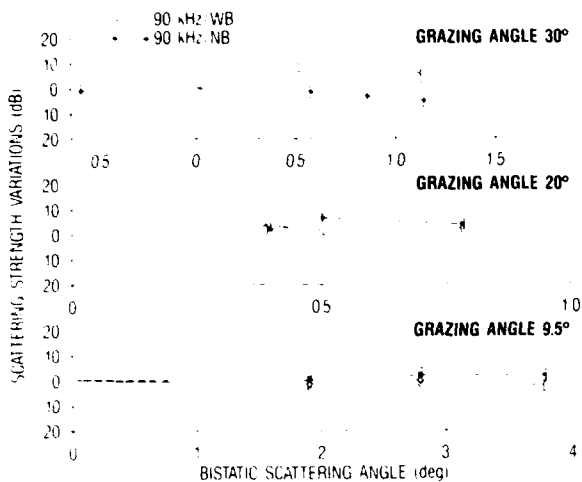


FIG. 12. Beamwidth dependence of vertical bistatic scattering variations at 90 kHz.

tions measured at Panama City did not always decrease with decreasing grazing angle. At a grazing angle of 20°, the range of variations was larger than the bistatic variations at grazing angles of 30° and 9.5°. The frequency dependence of the Panama City bistatic data at a grazing angle of 30° had a negative frequency dependence. At this time, the reasons for this negative frequency dependence and for the large bistatic variations at 20° are not clear. Generally, the bistatic results measured at Panama City were 1 to 5 dB higher than the Jacksonville results.

The difference in bistatic scattering variations measured using the 90-kHz/NB and 90-kHz/WB sources can be attributed to the difference in the size of the insonified area and the difference in the number of the individual scatterers in each area. At each grazing angle, the small areas insonified by the 90-kHz/NB source had few individual scatterers that would tend to cause significant bistatic scattering effects. As suggested by Stanic *et al.*,<sup>10</sup> the decrease in bistatic scattering strength variations as a function of range (except the horizontal results at 20°) may also be linked to the small sizes of the individual scatterers. As the acoustic wavelengths became larger and the grazing angles decreased, the seafloor began to appear smooth and thus may have had less effect on the angular scattering of the acoustic energy.

Urick<sup>7</sup> found that for another sandy area off Panama City, FL, there was a maximum of 10-dB variation in the bistatic scattering levels as a function of bistatic angle at 22 kHz. The variations at our Panama City site were significantly larger than 10 dB. Only at frequencies below 90 kHz

and at grazing angles less than 20° were the variations 10 dB or less. The results presented in this paper, and in Ref. 10, clearly demonstrated that the bistatic mechanisms are complex and have not been clearly identified.

#### ACKNOWLEDGMENTS

The authors would like to thank R. H. Love and R. W. Farwell of NOARL for their helpful comments. This work was supported by the Office of Naval Research, program element 61153N through the NOARL Defense Research Sciences Program and the Office of Naval Technology, program element 62435N. NOARL contribution number 243:052:91.

- <sup>1</sup>C. M. McKinney and C. D. Anderson, "Measurements of backscattering of sound from the ocean bottom," *J. Acoust. Soc. Am.* **36**, 158-163 (1964).
- <sup>2</sup>H. Boehme, N. P. Chotiros, L. D. Rolfeigh, S. P. Pitt, A. L. Garcia, T. G. Goldsberry, and R. A. Lamb, "Acoustic backscattering at low grazing angles from the ocean bottom. Part 1: Bottom backscattering strengths," *J. Acoust. Soc. Am.* **77**, 962-979 (1985).
- <sup>3</sup>D. J. Jackson, A. M. Baird, J. J. Crisp, and P. A. G. Thompson, "High-frequency bottom backscattering measurements in shallow water," *J. Acoust. Soc. Am.* **80**, 1188-1199 (1986).
- <sup>4</sup>N. P. Chotiros and H. Boehme, "High-frequency environmental acoustic bottom backscattering analysis," ARL-TR-86-27, Applied Research Laboratories, University of Texas at Austin (October 1986).
- <sup>5</sup>S. Stanic, K. B. Briggs, P. Fleischer, R. F. Ray and W. B. Sawyer, "Shallow-water high-frequency bottom scattering off Panama City, Florida," *J. Acoust. Soc. Am.* **83**, 2134-2144 (1988).
- <sup>6</sup>S. Stanic, K. B. Briggs, P. Fleischer, W. B. Sawyer, and R. F. Ray, "High-frequency acoustic backscattering from a coarse shell ocean bottom," *J. Acoust. Soc. Am.* **85**, 125-136 (1989).
- <sup>7</sup>A. W. Nolle, W. A. Hoyer, J. F. Mifsud, W. R. Runyan, and M. B. Ward, "Acoustical properties of water-filled sands," *J. Acoust. Soc. Am.* **35**, 1394-1408 (1963).
- <sup>8</sup>R. J. Urick, "Side scattering of sound in shallow-water," *J. Acoust. Soc. Am.* **32**, 351-355 (1960).
- <sup>9</sup>R. J. Urick, "Reverberation-derived scattering strength of the shallow sea bed," *J. Acoust. Soc. Am.* **48**, 392-397 (1970).
- <sup>10</sup>S. Stanic, E. Kennedy, and R. I. Ray, "Variability of shallow-water bistatic bottom backscattering," *J. Acoust. Soc. Am.* **90**, 547-553 (1991).
- <sup>11</sup>X. Zabal, M. H. Brill, and J. I. Collins, "Frequency and angle spreads of acoustic signals reflecting from a buried rough boundary," *J. Acoust. Soc. Am.* **79**, 673-680 (1986).
- <sup>12</sup>J. J. Martin, "Multipath reflections from a random surface," *J. Acoust. Soc. Am.* **47**, 1303-1309 (1968).
- <sup>13</sup>J. M. Restrepo and S. T. McDaniel, "Two models for the spatially covariant field scattered by randomly rough pressure release surfaces with Gaussian spectra," *J. Acoust. Soc. Am.* **87**, 2033-2043 (1990).
- <sup>14</sup>D. D. Ellis and D. V. Crowe, "Bistatic reverberation calculations using a three-dimensional scattering function," *J. Acoust. Soc. Am.* **89**, 2207-2214 (1991).
- <sup>15</sup>S. Stanic, K. B. Briggs, P. Fleischer, R. I. Ray, and W. B. Sawyer, "Shallow-water high-frequency bottom scattering off Panama City, Florida," *J. Acoust. Soc. Am.* **83**, 2134-2144 (1988).
- <sup>16</sup>S. Stanic, P. Fleischer, K. B. Briggs, M. P. Richardson, and B. Eckstein, "High-frequency acoustic bottom scattering experiments, Part I: Instrumentation and methods," NORDA Rep. No. 178, Naval Ocean Research and Development Activity, NSTL Station, MS (January 1987).